Available online at www.sciencedirect.com
SCIENCE DIRECT®
Journal of Solid State Chemistry 178 (2005) 2292–2300
JOURNAL OF SOLID STATE CHEMISTRY
www.elsevier.com/locate/jssc

Synthesis and characterizations of anion exchange organic–inorganic hybrid materials based on poly(2,6-dimethyl-1,4-phenylene oxide) (PPO)

Shaoling Zhang[a], Cuiming Wu[a], Tongwen Xu[a,*], Ming Gong[b], Xiaolong Xu[a]

[a]*Laboratory of Functional Membrane, School of Chemistry and Material Science, University of Science and Technology of China, Hefei 230026, PR China*

[b]*Laboratory for Materials Behavior and Design in USTC, Chinese Academy of Science, Hefei 230026, PR China*

Received 14 January 2005; received in revised form 8 May 2005; accepted 12 May 2005

Abstract

A series of poly(2,6-dimethyl-1,4-phenylene oxide) (PPO)-based organic–inorganic hybrid materials for anion exchange were prepared through sol–gel process of polymer precursors PPO–$Si(OCH_3)_3$. PPO–$Si(OCH_3)_3$ were obtained from the reaction of bromomethylated PPO with 3-aminopropyl-trimethoxysilane (A1110). These polymer precursors then underwent hydrolysis and condensation with additional A1110 to generate hybrid materials. The reaction to produce polymer precursors was identified by FTIR; while FTIR, TGA, XRD, SEM, as well as conventional ion exchange capacity (IEC) measurements were conducted for the structures and properties of the prepared hybrids. TGA results show that this series of hybrid materials possess high thermal stability; XRD and SEM indicate that the prepared hybrid materials are amorphous and the inorganic and organic contents show good compatibility if the ratio between them is proper. The IEC values of the hybrid materials due to the amine groups range from 1.13 mmol/gBPPO (material i) to 4.80 mmol/gBPPO (material iv).

Keywords: Organic–inorganic; Hybrid material; Sol–gel; PPO; Anion exchange material

1. Introduction

As early as the late 1980s, molecular level combination between organic polymers and inorganic materials has been of interest [1,2]. The resulting materials, i.e. the organic–inorganic hybrid materials have attracted great attention since then in the field of material science because of their unique opportunity to combine the remarkable features of organic compounds with those of inorganic materials [3–9] Their applications have been explored and reported in the fields of catalyst [10,11], coatings [12,13], gas permselectivity [14,15], fuel cell [16–18], chemical sensors [14], and ion-facilitated transport or ion exchange [14,19–21].

The interfacial force between the inorganic and organic phases of hybrid materials plays a major role in controlling the microstructures and the properties of the materials. It was observed that to disperse inorganic oxides, such as silica, uniformly in organic matrix, weak interactions or covalent bond would be formed between inorganic and organic components. Usually covalent bond would result in a more homogeneous system, so a significant feature to enhance the compatibility in the hybrid materials is the formation of covalent bond between the two components [22]. One route for forming such covalent-bonding hybrid materials is to functionalize organic polymer backbone with pending or terminal trialkoxysilyl ($Si(OR)_3$) groups. These

*Corresponding author. Fax: +86 551 3601592
E-mail address: twxu@ustc.edu.cn (T. Xu).

0022-4596/$ - see front matter © 2005 Elsevier Inc. All rights reserved.
doi:10.1016/j.jssc.2005.05.007

functionalized polymers can then undergo hydrolysis and condensation in a sol–gel reaction system with or without a coupling agent such as tetraethoxysilane (TEOS). There have been some reports that intermediate species of silanol groups derived from $Si(OR)_4$ and/or from $Si(OR)_3$ in the polymers condense with each other to produce chemically bonded homogeneous hybrid materials [22–25].

Among the varieties of hybrid materials explored, the ones that possess ion exchange properties have recently drawn particular interest since ion exchange is important for a variety of applications such as water treatment, chemical separation, and electrochemical sensing [26]. With these considerations, anion or cation exchange organic–inorganic hybrid materials or membranes based on polyethylene oxide (PEO) or poly(methyl acrylate) (PMA) have recently been explored in our laboratory [24,25,27]. To enrich the varieties in such kinds of hybrid materials, in this paper, we try to synthesize series of anion exchange organic–inorganic hybrid materials based on poly(2,6-dimethyl-1,4-phenylene oxide) (PPO). Here we chose PPO as the organic component, mainly due to the following two reasons: one is that PPO, characterized by a high glass transition temperature ($T_g = 212\,^{\circ}C$) and good thermal stability under nonoxidizing conditions, is one of the most widely used engineering plastics [28]; the other is that the bromination of PPO has been comprehensively conducted to develop a series of novel anion exchange polymeric membranes in our laboratory [29–31]. To prepare the hybrid materials, in this work bromomethylated PPO reacted with 3-aminopropyl-trimethoxysilane (A1110). The obtained polymer precursors then underwent hydrolysis and condensation together with additional A1110 in the presence of aqueous HCl catalyst. The properties of the hybrid materials thus obtained are reported and discussed.

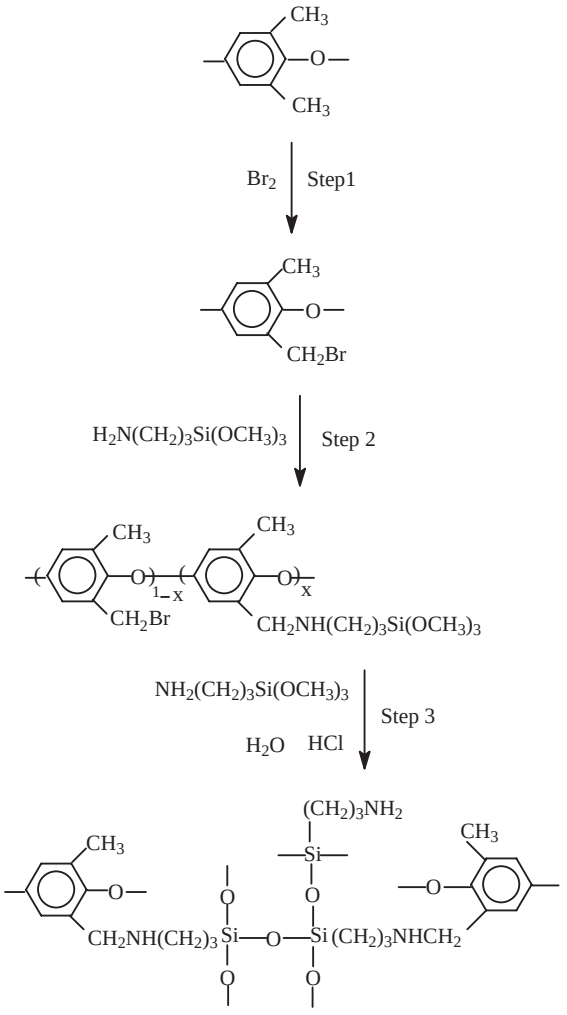

Scheme 1. The step reactions for preparing hybrid materials: Step 1. Bromination of PPO; Step 2. Synthesis of alkoxysilane-containing polymer precursors; Step 3. Preparation of organic–inorganic hybrid materials by sol–gel process.

2. Experimental

2.1. Materials

PPO of intrinsic viscosity equal to 0.57 dL/g in chloroform at 25 °C (molecular weight is about 90,000) was obtained from the Institute of Chemical Engineering of Beijing (China); Chlorobenzene, dimethyl formamide (DMF), and *n*-hexane are used after dehydrating by molecule sieves. A1110 was of analytical grade and was used as received.

2.2. Synthesis of hybrid materials

There are three steps in synthesizing the hybrid materials:

2.2.1. Bromination of PPO

Reaction procedure for bromination of PPO was described in detail in our previous papers [29,31]. PPO was dissolved in chlorobenzene to form a 10% (W/V) solution and this solution was subjected to bromination by adding chlorobenzene-diluted bromine. The molar of bromine being added was equal to that of PPO to control the extent of bromination and the reaction temperature ranges from 130 to 140 °C to control the substitution position (benzyl). The benzyl substitution ratio was calculated to be 0.8 through the ^1H NMR spectrum of BPPO, product of Step 1 in Scheme 1.

2.2.2. Preparation of polymer precursors $PPO-Si(OCH_3)_3$

This reaction was carried out under nitrogen atmosphere in a three-necked round-bottomed flask, which was equipped with a stirrer. BPPO was first dissolved in

Table 1
Compositions and thermal properties of the polymer precursors and the prepared hybrid materials

Sample code	BPPO	i	ii	iii	iv
Weight ratio of A1110η[a] in feed composition	0	31.0	37.5	47.4	64.3
x values calculated from the residue[b]	/	0.43	0.53	0.78	1.14
x values from initial feed composition[c]	/	0.50	0.67	1.0	1.0
Mole ratio of Si to phenyl in the polymer precursor	/	0.34	0.42	0.62	0.91
Residue[d] in TGA (wt%)					
Polymer precursor	3.24	11.52	13.62	21.31	26.50
Hybrid material	3.24	12.88	15.11	23.17	30.03
The highest decomposition temperature (°C)of the hybrids					
First	293	300/406	352	356	366
Second	496	560	561	562	588

[a]Weight ratio of A1110 in feed composition $\eta =$ [weight of A1110]/[weight of A1110 + weight of BPPO].
[b]x values were calculated according to the residual content of polymer precursors assuming that all the –Si(OCH_3) groups in the polymer precursors changed to silica and no other component remained at 800 °C.
[c]Theoretical x values were calculated from the initial feed composition by assuming the complete reaction between A1110 and BPPO as shown in Step 2 of Scheme 1.
[d]Residual contents are obtained at 800 °C from TGA thermograms, which were performed at heating rate 10/min under air atmosphere.

the mixture solution of chlorobenzene and DMF (the volume ratio of chlorobenzene to DMF is 1:1) with the concentration of 5% (W/V). Then A1110 was added into the mixture solution. As shown in Table 1, the weight ratio of A1110, which is defined as $\eta =$ [weight of A1110]/[weight of A1110 + weight of BPPO], ranges from 31.0% to 64.3% with respect to BPPO. The mixture solution was stirred further for 24 h, then part of it was taken out, precipitated, and washed with *n*-hexane for several times to eliminate the unreacted A1110 and get the polymer precursor PPO–Si(OCH_3)$_3$ for structure characterizations. The rest of the reaction mixture was ready for the next step. The reaction for preparing polymer precursor was described as Step 2 in Scheme 1.

2.2.3. Preparation of the hybrid materials

Into the reaction mixture got in Step 2, HCl solution (0.001 mole/mol water) was added (H_2O:HCl: alkoxides = 1:0.001:1, molar ratio) with violent stirring at room temperature under air atmosphere. After stirring for 1 h, the obtained casting solution was dropped onto Teflon plate. After drying at room temperature for 1 day, the plate was further dried at 100 °C for another day. When removed from the plate, final hybrid materials were obtained. The whole reaction steps were shown in Scheme 1 and the preparation procedures were summarized in Fig. 1.

Some hybrid films were also prepared for SEM observations by spin-coating the mixture solution (after 1 h of stirring) onto a silicon slice (1 cm × 1 cm), followed by the same drying procedure as mentioned above.

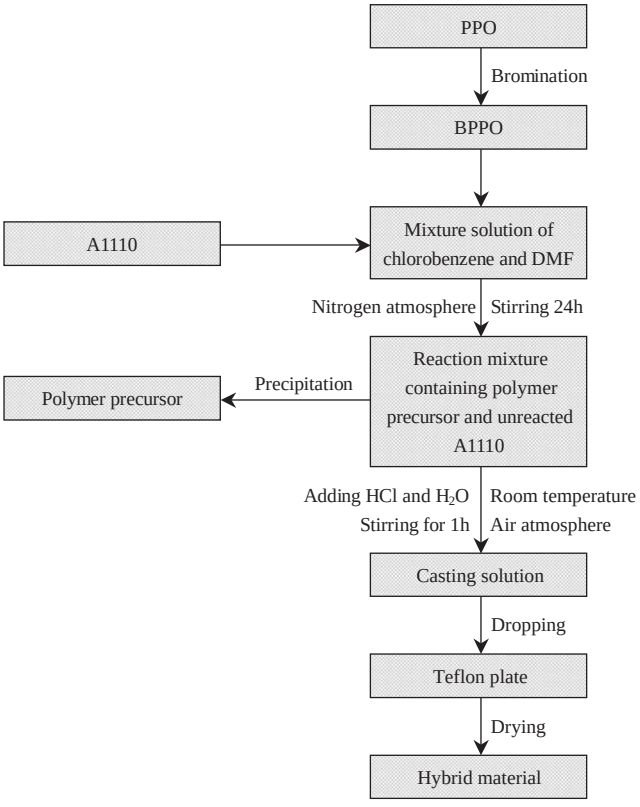

Fig. 1. Schematic diagram of the preparation procedure of the hybrid materials from PPO.

It should be pointed out that the nomenclature used in this paper is based on the difference in the content of A1110 in the feed composition (Step 2, Scheme 1). With an increase in A1110 content, the polymer precursors

and the corresponding hybrid materials were named as (i), (ii), (iii), and (iv), respectively as shown in Table 1.

2.3. Instrumentation and characterizations

The FT–IR spectra of the polymer precursors PPO–Si$(OCH_3)_3$ and hybrid materials were recorded from KBr pellets with a Magna-750 (American Nicolet Instrment Co.). Thermal behavior of the materials was determined by thermogravimetric analysis (TGA) (Shimadzu TGA-50H) under an air flow, with a heating rate of 10 °C/min . Crystallinity of the hybrid materials was conducted by the X-ray diffraction (XRD) technique, using Cu$K\alpha$ ($\lambda = 1.54178$ Å) radiation on a Japan Rigaku D/max-γA X-ray diffractometer. The morphologies of the hybrid materials were observed by an XL30-ESEM (Philips) environmental scanning electron microscopy.

The ion-exchange capacity (IEC) of the hybrid material was obtained according to the literature [32] and briefly described here. The materials are pre-equilibrated with 3 M NaCl, and rinsed with deionized water and then put into 1 M HCl to protonate the ammonium groups followed by washing with deionized water to remove excess HCl. The acid-free samples are immersed in 0.25 M NaOH for 1 day to deprotonate ammonium groups and collect the Cl^- ions; by deciding the generated Cl^- with ion-exchange chromatography (DIONEX, DX-120), anion exchange capacity values of the hybrids were obtained.

3. Results and discussion

3.1. FTIR for both the polymer precursors and the hybrid materials

As has been discussed in Section 2 and described in Fig. 1, the polymer precursors were got by eliminating the unreacted A1110 after the reaction of BPPO with A1110. Hybrid materials were obtained through the sol–gel process of polymer precursors together with unreacted A1110.

The structures of these PPO based polymer precursors and hybrid materials were characterized by FT–IR, and the results are presented in Fig. 2(a) for precursors and Fig. 2(b) for materials, respectively.

In Figs. 2(a) and (b), characteristic peaks contributing from PPO units are observed at 1604, 1466, 1302, and 1189 cm^{-1}, as analyzed in our previous report [30]. In the curves of the polymer precursors, the new absorption peaks appearing at about 1086 and 1028 cm^{-1} are associated with the v (Si–OCH_3) and linear v (Si–O–Si) vibration [33] coming from the A1110 that have reacted to the BPPO backbone. As to the linear Si–O–Si bond in the polymer precursors, it may be due to the following:

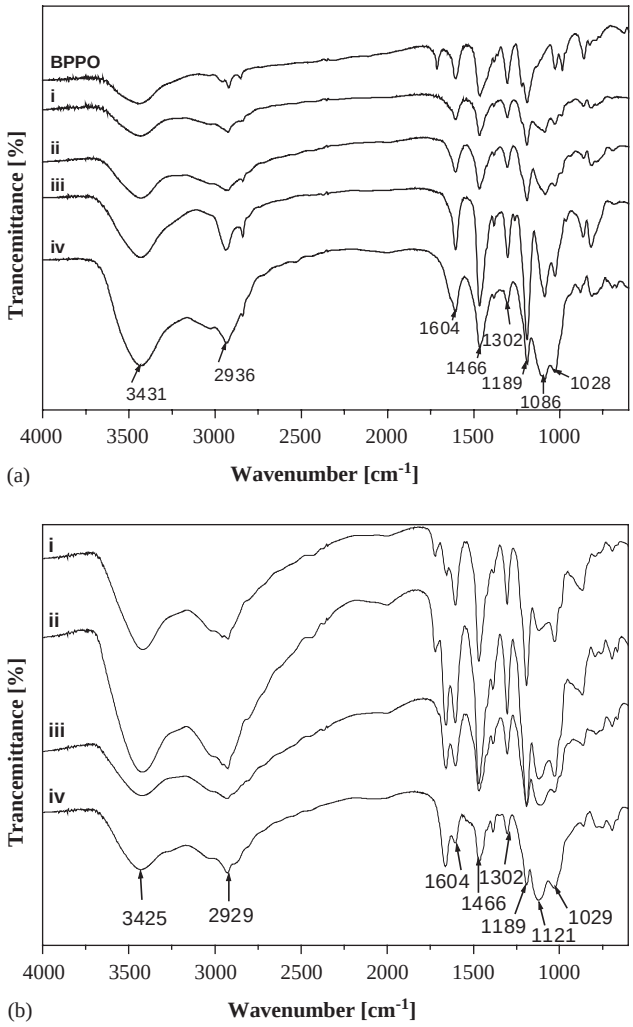

Fig. 2. FT–IR spectra for (a) polymer precursors and (b) hybrid materials.

during the reaction process of A1110 with BPPO, trace water vapor may be introduced into the reaction system, then the unstable Si$(OCH_3)_3$ groups was likely to hydrolyze and condense partly, resulting in such groups as $\equiv$Si–O–Si(OH)$(OCH_3)_2$. Similar phenomenon had been observed in the reaction system of PMA with *N*-[3-(trimethoxysilyl) propyl] ethylene diamine, as described by our previous paper [27]. What's more, the relative density of the peak at about 1086 cm^{-1} to that at 1189 cm^{-1}, which is due to the ether band of BPPO, becomes stronger with the increase of A1110 in the feed composition. This can be explained that with the increase of A1110 content, more A1110 reacted with BPPO. In Fig. 2(b), the adsorption peak at about 1086 cm^{-1} disappeared and new absorption peaks at 1121 cm^{-1} appeared, which can be due to the formation of silica networks from the sol–gel process.

It should be pointed out that the obtained polymeric precursors are insoluble and the solid state NMR is not available at this moment, it is difficult to quantitatively

confirm the structure and composition of the polymer precursors. However, some indirect proofs can be found for this synthesis. Discussion of the FTIR spectra of the polymer precursors above has shown that A1110 was actually successfully connected to BPPO chains in the polymer precursor. Such reaction can also be proved by the subsequent SEM comparison between the hybrid materials and the specially prepared sample as shown in Section 3.5 (Fig. (6)). Also, in the literatures, the reaction between polymers containing chloromethylated groups and different kinds of amines with high steric hindrance has been successfully conducted [32,34–37]. So it can be inferred that the reaction between $-CH_2Br$ and $-NH_2$ in our work (as shown in Scheme 1 Step 2) is relatively easy to happen. The amount of the A1110 connected to BPPO in the polymer precursors would be roughly measured through the subsequent TGA data as discussed in the next section.

3.2. TGA analysis

3.2.1. TGA for the polymer precursors

The thermal stability of the polymer precursors were measured by means of TGA under air atmosphere and the results are shown in Fig 3. For comparison, TGA measurement was also conducted for BPPO, and the result is shown in Fig 3, too.

From Fig. 3, it can be seen that compared with BPPO, the polymer precursors show no obvious enhancement in thermal stability. The possible reason may be that silica network had not been formed yet in the precursors. Section 3.2.2 will give further discussion about this. Our main interest in the TGA results of the polymer precursors is their residual content at 800 °C. Assuming that all the $-Si(OCH_3)$ groups in the polymer precursors changed to silica and no other component remained at 800 °C [25], it is possible to determine the amination degree of BPPO, i.e. x value in Scheme 1 through the residue in TGA, and the results were collected in Table 1. The theoretical x value can be calculated from the initial feed composition by assuming the complete reaction and also was listed in Table 1. It is demonstrated that in most cases, the x values calculated from the residues are less than the theoretical calculations, indicating that after the reaction of BPPO with A1110 as shown in Step 2 of Scheme 1, there is still some unreacted A1110 in the reaction bottle. These unreacted A1110 will attend the sol–gel process together with the polymer precursors, as shown in Step 3 of Scheme 1.

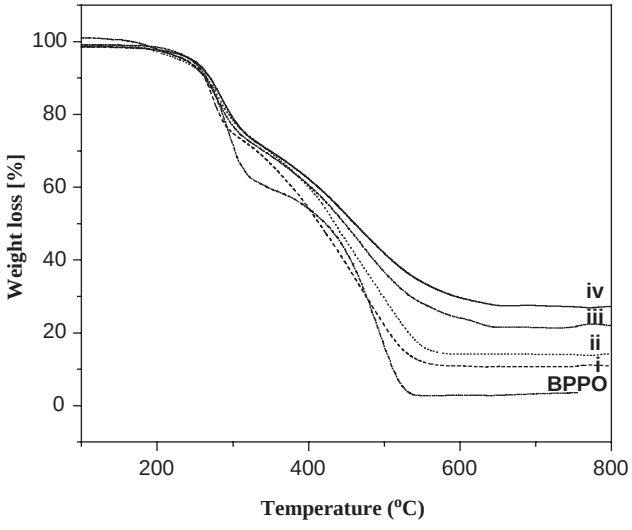

Fig. 3. TGA thermograms of polymer precursors.

It is noted that there exists some errors for the calculated x values from the residues of polymer precursors because some organic moiety may be trapped in the inorganic matrix at 800 °C, especial for the cases that the inorganic content becomes higher. This may be the reason why the x value calculated from the residue for the last sample is higher than that calculated from the initial feed composition. But such an error does not affect any conclusion obtained in this section [25].

From the x values and the benzyl substitution ratio, the molar ratio of Si to phenyl in the polymer precursor can be calculated, and the result has been listed in Table 1. As theoretically expected, the molar ratio of Si to phenyl in polymer precursor increases with the increase of A1110 content in the feed composition. Then it can be concluded that more A1110 was connected to the polymer backbone covalently when more A1110 existed in the reaction system.

3.2.2. TGA for the hybrid materials

The thermal stability of the prepared hybrid materials were also measured by means of TGA under air atmosphere and the results are shown in Fig 4 together with that of BPPO.

From Fig. 4(a) it can be seen that in the beginning part of the heating process (<200 °C), the degradation degree of the prepared hybrid materials is higher than that of BPPO. This can be explained that after sol–gel process, more A1110 was introduced in the prepared hybrid materials, and the thermal stability of the long carbon chain from A1110 is not so good as that of BPPO. However, during the rest heating process (250–800 °C) this series of hybrid materials exhibit much higher thermal stability, which is manifested in generally higher temperatures where the hybrids reached the highest decomposition slope. This improvement of the thermal stability of the hybrids was most probably due to the newly formed silica network after the sol–gel process.

It can also be observed that the thermal degradation behaviors were divided into two stages. To show these stages more clearly, DrTGA results were displayed in Fig. 4(b). It can be seen that both BPPO and the

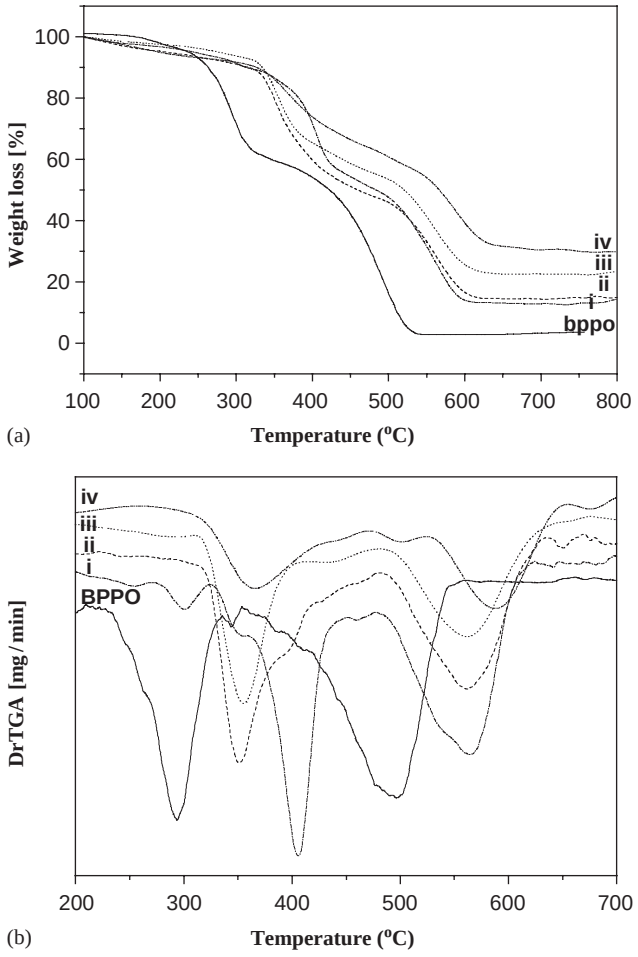

Fig. 4. (a) TGA and (b) DrTGA thermograms of hybrid materials.

prepared hybrid materials possess two weight loss peaks. Consulting these TGA observations and those of other hybrid materials containing similar components [38–40], here, the primary degradation stage could be caused by the decomposition of ammonium groups, methyl and ether groups of BPPO and the carbon chain contributing from A1110, and the secondary degradation stage could be brought about by the splitting of residue of BPPO and further oxidation of silicate. As shown in Table 1, with an increase in inorganic content in the prepared hybrid materials, temperatures for both the first weight loss peak and the second one increase as theoretically expected. But an exception was found for material (i), there appears two peaks for the first weight loss as shown in Fig. 4(b): one is at around 300 °C which is very close to that of BPPO, and the other is at around 406 °C which is higher than those of the other hybrid materials. Because at this case, the A1110 content is quite small, thus much unreacted BPPO is left in the hybrids. Therefore, the peak at 300 °C corresponds to the unreacted BPPO while the peak at 406 °C maybe corresponds to the silanol groups that failed to form the silica network in the sol–gel process due to the relatively low content of A1110 in the feed composition.

While comparing the residual content of polymer precursors with that of the corresponding hybrid materials, it can be seen that the difference becomes more and more obvious with the increase of A1110 content in the feed. This can be ascribed to the part of A1110 that did not react with BPPO but was introduced in the prepared hybrid materials by attending the sol–gel process (as discussed in Section 3.2.1). For materials i and ii, the difference is little, because the A1110 content is relatively small in the feed, and most of them could be connected to the polymer chain after the reaction as shown in Step 2. But for material iv, the content of A1110 in the feed was more than the amount that the reaction of Step 2 required, then only part of it could attend the reaction with BPPO, so the difference is the biggest among the prepared four materials.

3.3. IEC of the prepared hybrid materials

Anion exchange capacity measurements were conducted for the prepared hybrid material and the results were shown in Table 2. Considering the change in the hybrids' molecular weight with the change of the feed composition, IEC values were calculated as the mmol of exchangeable ions per gram of BPPO; namely, BPPO is chosen as the standard for calculation of IEC. As can be seen in Table 2, the anion-exchange capacities of the prepared hybrid materials increase from 1.13 mmol/g BPPO (material (i)) to 4.80 mmol/g BPPO (material (iv)). This increasing trend is due to an increase in A1110 content, and thus the increase in the ammonia groups from A1110. When the unit of IEC values was roughly converted to mmol/g material, the values are in the range of around 0.8 (material (i))—around 1.7 (material (iv)) mmol/g material. Compared with other ion exchange materials or membranes in literature [25,32,41–43], the IEC value of these prepared hybrid material is moderate.

3.4. XRD for the prepared hybrid materials

XRD measurements were conducted to estimate the crystallinity of the prepared hybrid materials. All the samples were ground into fine powder for the measurement and the results are shown in Fig. 5. It can be seen

Table 2
Anion-exchange capacities (IEC) of the prepared hybrid materials (mmol/gBPPO)

Sample code	i	ii	iii	iv
IEC values	1.13	1.69	2.97	4.80

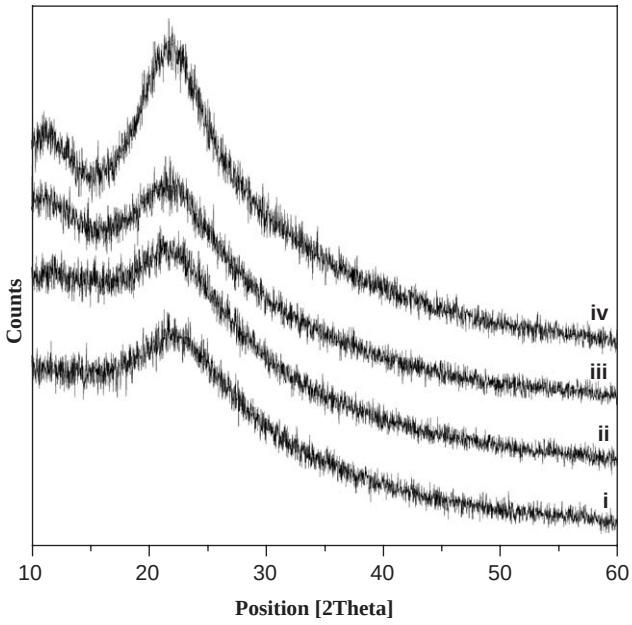

Fig. 5. X-ray diffractograms of hybrid materials.

that the diffractogram is typical of being amorphous despite the existence and change of inorganic content. So it can be inferred that all the hybrid materials prepared in this way are amorphous, which is in accordance with our previous work [25].

3.5. Morphology study of the hybrid materials

As is known, the compatibility between the organic and inorganic component has a great effect on the thermal, mechanical and optical properties of the hybrid materials. So SEM was conducted in this work to investigate the distribution of silica and microphase separation in the hybrid materials. Figs. 6(a)–(d) demonstrated the surface morphologies of the prepared hybrid material (i)–(iv), respectively. It is shown that the surface morphology varies with the inorganic content in the hybrids and white silica particles that show the degree of phase separation increase with the content of A1110 in the feed. For example, in Figs. 6(a) and (b), few white silica particles could be found to disperse in

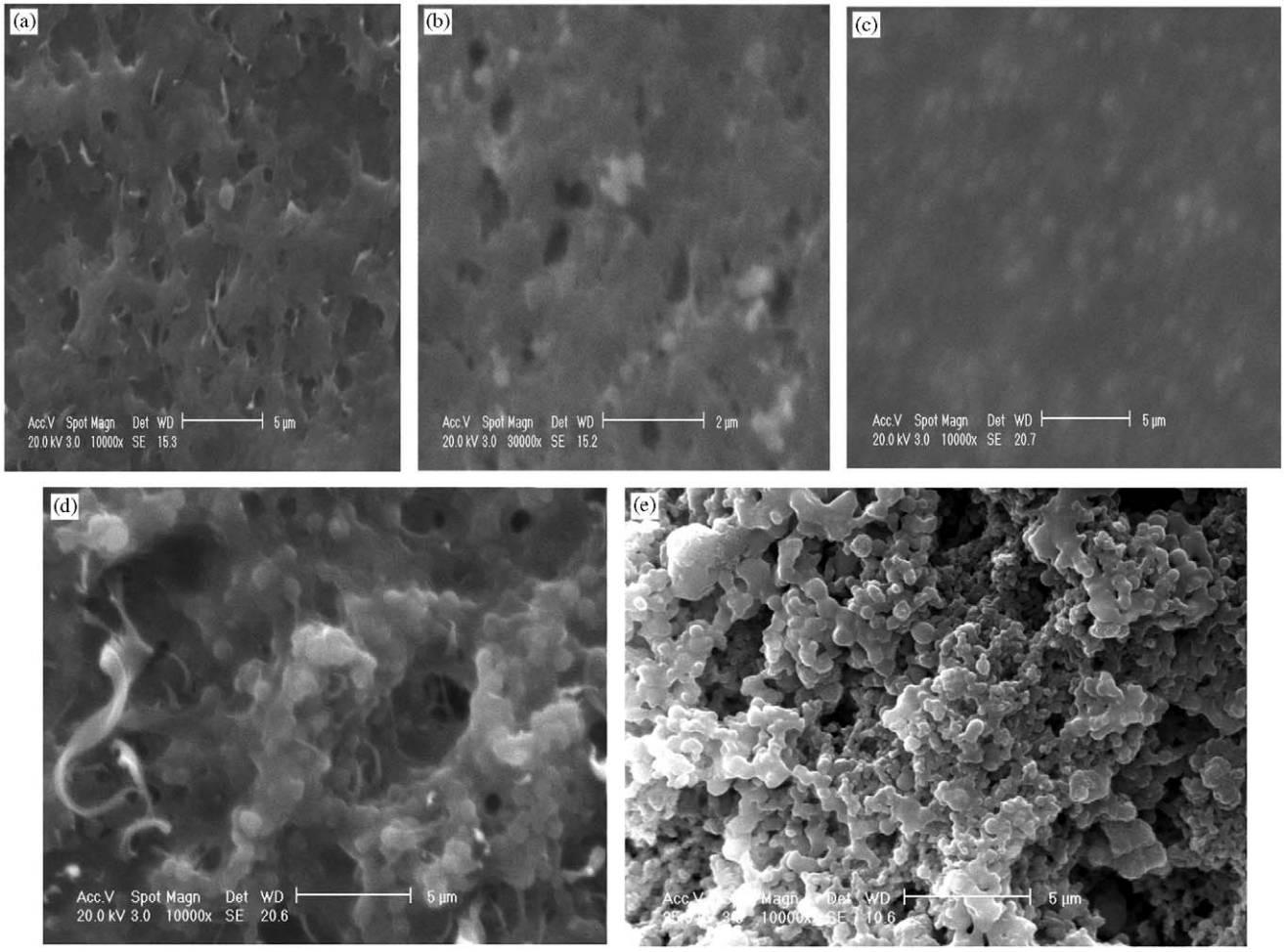

Fig. 6. SEM photograph of the prepared hybrid materials (a) i, (b) ii, (c) iii, (d) iv, and (e) reference sample.

the polymer matrix; in Fig. 6(c), although not very clear, more small white particles can be seen to disperse in the prepared material; while in Fig. 6(d), obvious silica particles appear on the surface. The reason may be that silica content in the hybrid materials tends to increase with an increase in content of A1110 in the feed. Especially for material iv, the content of A1110 in the feed was more than the reaction between A1110 and BPPO theoretically needed, so part of the A1110 could not connect to the BPPO chains through a covalent bond, but only attend the sol–gel process to form a silica network, which has been discussed in Section 3.2. It is the presence of an excess silica content in the hybrid material that causes the separation between the organic and inorganic phases, and deteriorates the compatibility between the silica network and the polymer chain. Therefore, from the viewpoint of the compatible degree of the hybrids, the ratio of organic and inorganic content in the feed composition should be controlled within a limit value for preparation of practical hybrid materials.

Additionally, to prove the formation of covalent bond in the hybrid materials or the reaction between A1110 and BPPO, a reference sample was prepared by directly mixing A1110 with PPO (with mol ratio 1:1) in the mixture solution of chlorobenzene and DMF, then undergoing the sol–gel process and drying procedures as the four hybrid materials. As a comparison, SEM result of this sample is shown in Fig. 6(e). Compared with those of the prepared hybrid materials, significantly large difference can be seen. In Fig. 6(e), much more particles can be observed. Instead of dispersing uniformly, these particles stack and pileup and there is no orderliness in them. Because there is no reaction happening between PPO and A1110 in the reference sample, so the organic and inorganic phases are connected mainly by the hydrogen bonding. Then the role the covalent bond plays in the prepared hybrid material is very obvious: the inorganic and organic phases showed better compatibility in the prepared hybrid materials than in the reference sample. As described earlier, SEM comparison here can give a strong evidence that the reaction between A1110 and BPPO actually occurred.

To sum up, the SEM results coincided with the fact that the compatibility of the inorganic and organic phases in hybrid materials can be enhanced via connecting polymer matrix with inorganic silica covalently [23], and the degree can be controlled by adjusting the ratio of organic and inorganic content in the feed composition.

4. Conclusions

In this article, a series of silica-containing anion exchange hybrid materials were prepared by reacting A1110 with BPPO and then forming silica network by sol–gel process. FT–IR, TGA, XRD, SEM as well as IEC measurements were conducted for the polymer precursors and/or hybrid materials. The results reveal that the prepared hybrid materials are amorphous and bear better miscibility than inorganic–organic blend materials. What's more, the prepared hybrid materials possess better thermal stability than usual organic ion exchange materials which are often limited under 80 °C [44]. Due to the good thermal stability and the anion exchange capacity, this kind of hybrid materials are expected to be used as separation membranes, adsorption or ion exchange materials for a variety of applications such as water treatment, chemical separation, etc.

Acknowledgments

This job was supported in part by Program for New Century Excellent Talents in University (No. NCET-04-0583), National Basic Research Program of China (973 Program, No. 2003CB615700) and the National Science Foundation of China (No. 20376079).

References

[1] G.L. Wilkes, B. Orler, H. Huang, Polym. Prepr. 26 (1985) 300.
[2] C.S. Parkhurst, L.A. Doyle, L.A. Silverman, Mater. Res. Soc. Symp. Proc. 73 (1986) 769.
[3] Y. Chujo, T. Saegusa, Adv. Polym. Sci. 100 (1992) 11.
[4] B. Novak, Adv. Mater. 5 (1993) 422.
[5] J. Livage, B. Mater. Sci. 22 (1999) 201.
[6] Y.G. Hsu, K.H. Lin, I.L. Chiang, Mater. Sci. Eng. B 87 (2001) 31.
[7] L. Cantu, G. Romero, J. Solid State Chem. 147 (1999) 601.
[8] Z.H. Huang, K.Y. Qiu, Polymer 38 (1997) 521.
[9] L.H. Lee, W.C. Chen, Chem. Mater. 13 (2001) 1137.
[10] M. Petrucci, D. Fenwick, A. Kakkar, J. Mol. Catal. A: Chem. 146 (1999) 309.
[11] K. Dallmann, R. Buffon, Catal. Commun. 1 (2000) 9.
[12] Y. Du, M. Damron, G. Tang, Prog. Org. Coat. 41 (2001) 226.
[13] S. Dire, F. Babonneau, C. Sanchez, J. Livage, J. Mater. Chem. 2 (1992) 239.
[14] C. Guizard, A. Bac, M. Barboiu, N. Hovnanian, Sep. Purif. Technol. 25 (2001) 167.
[15] M. Iwata, T. Adachi, M. Tonidokoro, J Appl. Polym. Sci. 88 (2003) 1752.
[16] D.H. Jung, S.Y. Cho, D.H. Pech, J. Power Sources 106 (2002) 173.
[17] L. Tchicaya-Bouckary, D.J. Jones, J. Rosiere, Fuel Cells 1 (2002) 40.
[18] I. Honma, O. Nishikawa, T. Sugimoto, S. Nomura, H. Nakajima, Fuel Cells 2 (2002) 52.
[19] P. Lacan, C. Guizard, P. Le Gall, J. Membr. Sci. 100 (1995) 99.
[20] M. Barboiu, C. Luca, C. Guizard, J. Membr. Sci. 129 (1997) 197.
[21] V. Barboiu, M. Barboiu, J. Membr. Sci. 204 (2002) 97.
[22] G. Kickelbick, Prog. Polym. Sci. 28 (2003) 83.
[23] I. Honma, S. Hirakawa, K. Yamada, J.M. Bae, Solid State Ion. 118 (1999) 29.
[24] C.M. Wu, T.W. Xu, W.H. Yang, J. Membr. Sci. 216 (2003) 269.

[25] C.M. Wu, T.W. Xu, W.H. Yang, J. Solid State Chem. 177 (2004) 1660.
[26] P. Tien, L.K. Chau, Y.Y. Shieh, Chem. Mater. 13 (2001) 1124.
[27] C.M. Wu, T.W. Xu, W.H. Yang, Eur. Polym. J. 40 (2005) 1901.
[28] Y. Pan, Y.H. Huang, B. Liao, et al., J. Appl. Polym. Sci. 61 (1996) 1111.
[29] T.W. Xu, W.H. Yang, J. Membr. Sci. 190 (2001) 159.
[30] T.W. Xu, F.F. Zha, J. Membr. Sci. 199 (2002) 203.
[31] B.B. Tang, T.W. Xu, M. Gong, W.H. Yang, J. Membr. Sci. 248 (2005) 119.
[32] E.N. Komkova, D.F. Stamatialis, H. Strathmann, M. Wessling, J. Membr. Sci. 244 (2004) 27.
[33] K.T. Adjemian, S.J. Lee, S. Srinivasan, J. benziger, A.B. Bocarsly, J. Electrochem. Soc. 149 (3) (2002) A258.
[34] T. Sata, K. Teshima, T. Yamaguchi, J. Polym. Sci. Pol. Chem. 34 (1996) 1475.
[35] T. Sata, T. Yamaguchi, K. Matsusaki, J. Phys. Chem. 99 (1995) 12875.
[36] A.K. Pandey, A. Goswami, D. Sen, S. Mazumder, R.F. Childs, J. Membr. Sci. 217 (2003) 117.
[37] T. Sata, Y. Yamane, K. Matsusaki, J. Polym. Sci. Polym. Chem. 36 (1998) 49.
[38] B. Smitha, S. Sridhar, A. Khan, J. Membr. Sci. 225 (2003) 63.
[39] X.G. Li, J. Appl. Polym. Sci. 71 (1999) 1887.
[40] S.H. Goh, S.Y. Lee, Thermochim. Acta. 120 (1987) 293.
[41] J.F. Blanco, Q.T. Nguyen, P. Schaetzel, J. Membr. Sci. 186 (2001) 267.
[42] T.W. Xu, Z.M. Liu, W.H. Yang, J. Membr. Sci. 249 (2005) 183.
[43] R.K. Nagarale, G.S. Gohil, V.K. Shahi, R. Rangarajan, Macromolecules 37 (2004) 10027.
[44] J. Shi, Q. Yuan, C.J. Gao (Eds.), Handbook on Membrane Technology, Press of Chemical Industries, Bejing, China, 2001 (in Chinese).